

Kinetics of Chromium(III) Oxidation to Chromium(VI) by Reaction with Manganese Dioxide

L. Edmond Eary* and Dhanpat Rai

Battelle, Pacific Northwest Laboratories, Richland, Washington 99352

■ The kinetics of oxidation of aqueous Cr(III) to Cr(VI) by reaction with pyrolusite [β -MnO₂(s)] were studied in aerated and deaerated solutions at 27 °C for pH 3.0–10.1, for 10^{-4.7}–10^{-3.4} M Cr(III), and as a function of β -MnO₂(s) surface area to assess the possible effects on Cr transport in industrial waste materials. The oxidation of aqueous Cr(III) is not appreciably affected by dissolved oxygen, indicating that Cr(III) reacts directly with β -MnO₂(s) to produce Cr(VI) and not by catalyzed reactions with oxygen at the β -MnO₂(s) surface. In acidic solutions, the oxidation of aqueous Cr(III) is highly nonlinear with time, possibly because strong adsorption of the produced anionic Cr(VI) species limits the amount of Cr(III) species able to contact active oxidizing sites on the β -MnO₂(s) surface. The following expression is derived from the rate data for pH 3.0–4.7 that empirically account for the nonlinear rate by describing the reaction rate in terms of the fraction of Cr(VI) to total Cr, f_{Cr} , remaining in solution:

$$d f_{Cr} / dt \text{ (s}^{-1}\text{)} = k(A/V)[Cr_T]^{-1}(1.0 - f_{Cr})^{3.2(\pm 0.8)} \text{ for } f_{Cr} \leq 1.0$$

where $k = 2.0 (\pm 1.6) \times 10^{-13} \text{ mol}\cdot\text{m}^{-2}\cdot\text{s}^{-1}$, A/V is the β -MnO₂(s) surface area to solution volume ratio in $\text{m}^2\cdot\text{L}^{-1}$, and $[Cr_T]$ is the molar concentration of total dissolved Cr. In slightly acidic to basic solutions, the oxidation of aqueous Cr(III) is very slow and is limited by the low solubility of Cr(OH)₃(s).

Introduction

Chromium may be present in aqueous environments in either one or both of the Cr(III) and Cr(VI) oxidation states. The mobility of aqueous Cr(III) is expected to be limited in slightly acidic to basic waters by the low solubilities of Cr(OH)₃(s) and (Fe,Cr)(OH)₃(s) (1, 2). In contrast, the mobility of aqueous Cr(VI) is expected to be controlled primarily by adsorption and desorption reactions. To use the available data on precipitation and adsorption reactions for predicting the geochemical behavior of Cr, quantitative data are needed for the reactions that control the distributions of the aqueous Cr oxidation states. The high concentrations of Cr in some fly ash transport waters and boiler cleaning wastes (3) indicate that leaching of Cr from utility wastes and mobility in groundwaters may be of environmental concern.

Numerous reductants that could reduce Cr(VI) to Cr(III), such as ferrous iron (4), reduced sulfur species (5), and organic material (6), may exist in leaching environments. Of these reductants, ferrous iron is ubiquitous in both utility wastes and soils. However, with the exception of the manganese oxides and dissolved oxygen, there are no other generally occurring inorganic oxidants that conceivably could oxidize Cr(III) to Cr(VI) in most waste materials and soils. Manganese oxides have a high adsorption capacity for metal ions (7), thus potentially providing a local surface environment in soils and solid wastes in which the coupled processes of aqueous Cr(III) oxidation and manganese oxide reduction may take place. Bartlett and James (8) observed that Cr(III) was oxidized to Cr(VI) more readily in soils with high elemental contents of Mn

as compared to other soils. Schroeder and Lee (9) have shown that a significant fraction of the aqueous Cr(III) present in lake waters can be converted to Cr(VI) by reaction with an unspecified form of MnO₂(s). In other environments, such as seawater at pH 8.1, Nakayama et al. (10) found that Cr(III) was oxidized by MnOOH(s). Manganese oxides have also been shown to oxidize aqueous Co(II) to Co(III) (11) and aqueous As(III) to As(V) (12).

In this paper, we present experimental data on the kinetics of aqueous Cr(III) oxidation to Cr(VI) by reaction with pyrolusite [β -MnO₂(s)], primarily for acidic environments. We chose to use β -MnO₂(s) in this study because it is expected to be a primary Mn-containing solid in coal fly ashes and smelter wastes that are formed at high temperatures, although it does not form in soil environments. Additionally, β -MnO₂(s) is the most chemically pure and crystalline form of MnO₂(s) compared to soil forms such as birnessite [δ -MnO₂(s)] or cryptomelene [α -MnO₂(s)]. Consequently, β -MnO₂(s) can be expected to have a lower surface energy relative to the other manganese oxides. Thus, if Cr(III) is oxidized to Cr(VI) by reaction with β -MnO₂(s), then it is logical to assume that similar and probably more rapid reactions with other forms of manganese oxides are likely to occur.

Experimental Method

Materials. The manganese oxide used in the experiments was reagent-grade MnO₂(s) and was determined to be pyrolusite [β -MnO₂(s)] by powder X-ray diffraction. β -MnO₂(s) was sieved to obtain the 0.105–0.149-mm fraction. This fraction was washed repeatedly in deionized water, leached in a 10% HCl plus water solution for 20–30 min, and again repeatedly rinsed in deionized water. The purpose of the washing and preleaching of β -MnO₂(s) was to remove most of the dust-sized particles that commonly adhere to the surfaces of larger grains. The specific surface area of prepared β -MnO₂(s) was measured by N₂ gas adsorption and determined to be 5.7 (± 0.5) m²·g⁻¹ by Brunauer-Emmett-Teller (BET) calculation.

A 10^{-1.74} M Cr(III) stock solution that was made by dissolving CrCl₃·6H₂O(s) in 0.1 M HCl and a similar stock solution of Cr(VI) that was made with K₂Cr₂O₇(s) were used as the sources of Cr in the experiments. All chemicals used were of reagent grade, and distilled-deionized water was used in all experiments.

Experimental Conditions. The experiments were conducted to determine how the rate of aqueous Cr(III) oxidation is affected by dissolved oxygen, Cr(III) and Cr(VI) concentrations, β -MnO₂(s) surface area, and pH. Chromium(III) concentrations in the rate experiments ranged from 1.9 × 10⁻⁶ to 38.5 × 10⁻⁶ M, and the β -MnO₂(s) surface area to solution volume ratios (A/V) ranged from 0.7 to 71.4 m²·L⁻¹. The pH range of most experiments was limited to 3.0–4.7 because in more basic solutions aqueous Cr(III) is constrained to very low concentrations by the solubility of Cr(OH)₃(s) (1). We expected that the presence of a solubility-controlling phase would obscure the factors affecting the rate of aqueous Cr(III) oxidation; thus, most of the experiments were conducted in acidic solutions where the possible complications caused by Cr(OH)₃(s)

precipitation could be avoided. However, three experiments were conducted at pH values of 6.3, 8.3, and 10.1 to obtain a qualitative measure of the oxidation rate in the presence of $\text{Cr}(\text{OH})_3(\text{s})$. A complete listing of the experimental conditions and the Cr(III) oxidation rate data is available in Rai et al. (13).

Procedure. The rate experiments were conducted with 800 mL of solution in 1.0-L polyethylene bottles that were immersed in a constant 27 °C temperature bath. Air or argon that was scrubbed of $\text{CO}_2(\text{g})$ and saturated with water vapor was bubbled through the experimental solutions for 8–16 h before adding $\beta\text{-MnO}_2(\text{s})$ and continuously during the experiments. The continuous bubbling of the solutions served to keep dissolved oxygen concentrations constant and also thoroughly mixed the solutions without abrading the $\beta\text{-MnO}_2(\text{s})$ grains. Chromium concentrations were adjusted by adding an aliquot of the Cr stock solutions. The pH was adjusted to the starting value with 0.01 M HCl or NaOH. After the initial adjustment, the pH was not readjusted but never varied by more than ± 0.3 pH unit about the starting value. Experiments were started by adding a weighed amount of $\beta\text{-MnO}_2(\text{s})$ to the solutions, and solution samples were then periodically withdrawn for analyses. A total of 10–20 samples of 5–15 mL each were collected from an experiment over a time span of 8–800 h.

Analytical Methods. All solution samples were passed through 0.22- μm filters immediately after withdrawal from the reaction bottles. The concentrations of Cr(VI) were determined within 15 min after sampling by a colorimetric method using the diphenylcarbazide chromagen (14). Total dissolved Cr was also determined with diphenylcarbazide after all Cr(III) was oxidized to Cr(VI) with KMnO_4 (14). The Cr(III) concentrations were determined by difference. The analytical precision on replicate samples was $\pm 5\%$ for solutions that contained more than about 50 ppb Cr. Between 10 and 50 ppb, analytical precision decreased to about $\pm 25\%$. Dissolved Mn concentrations were determined by atomic absorption spectroscopy with an analytical precision on replicate samples of $\pm 10\%$ to a reliable detection limit of 50 ppb. Dissolved oxygen concentrations were determined with an oxygen probe that was standardized against atmospheric oxygen.

Results and Discussion

Dissolved Oxygen. The rate of oxidation of a 1.9×10^{-6} M Cr(III) solution by approximately 8.0 ppm dissolved oxygen was measured at pH 4.0, 12.0, and 12.5, but no aqueous Cr(VI) was detected in these solutions even after as long as 24 days. This result differs from that of Schroeder and Lee (9), who observed that 2–3% of a 2.4×10^{-6} M Cr(III) solution was very slowly oxidized to Cr(VI) by dissolved oxygen over a 2-week period in buffered solutions with pH 5.5–9.9 and in natural lake waters. From our results and those of Schroeder and Lee (9), we concluded that the oxidation of aqueous Cr(III) solely by dissolved oxygen was too slow to be considered a significant factor in further rate experiments with $\beta\text{-MnO}_2(\text{s})$. The effect of dissolved oxygen on the rate of oxidation of aqueous Cr(III) by $\beta\text{-MnO}_2(\text{s})$ at pH 4.0 was further evaluated by comparing reaction rates for solutions that were sparged with air (approximately 8.0 ppm dissolved oxygen) or argon (approximately 0.5 ppm dissolved oxygen) (Figure 1a). The oxidation rates in aerated solutions with surface area to solution volume ratio (A/V) of $7.1 \text{ m}^2\text{-L}^{-1}$ were slightly higher than in the comparable deaerated solutions, but in general, the differences in oxidation rates were very small (Figure 1a). Previous workers (12) have suggested that manganese oxide surfaces may catalyze

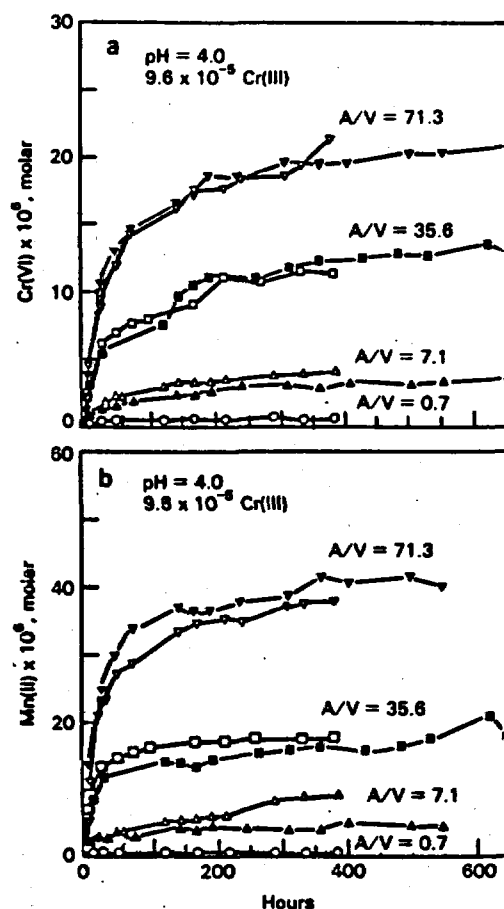


Figure 1. Effects of dissolved oxygen and $\beta\text{-MnO}_2(\text{s})$ surface area to solution volume ratio (A/V) on rates of (a) Cr(VI) formation and (b) $\beta\text{-MnO}_2(\text{s})$ dissolution for initial $[\text{Cr}(\text{III})] = 9.6 \times 10^{-6}$ M and pH 4.0. Open symbols represent aerated solutions, and solid symbols represent solutions that were deaerated with argon.

metal oxidation by dissolved oxygen. In contrast, our results (Figure 1a) show that dissolved oxygen does not greatly affect the rate of aqueous Cr(III) oxidation by $\beta\text{-MnO}_2(\text{s})$ and instead indicates that oxidation occurs by direct reaction with $\beta\text{-MnO}_2(\text{s})$.

Surface Area. The effects of the ratio of $\beta\text{-MnO}_2(\text{s})$ surface area to solution volume, given by A/V with units of $\text{m}^2\text{-L}^{-1}$, on the rates of aqueous Cr(III) oxidation and $\beta\text{-MnO}_2(\text{s})$ dissolution are also shown in Figure 1. An order of magnitude increase in the $\beta\text{-MnO}_2(\text{s})$ surface area resulted in nearly an order of magnitude increase in the amount of aqueous Cr(VI) produced by the oxidation of Cr(III) (Figure 1a). Similarly, the rate of $\beta\text{-MnO}_2(\text{s})$ dissolution was nearly directly proportional to the $\beta\text{-MnO}_2(\text{s})$ surface area (Figure 1b). The results in Figure 1a are typical of the oxidation rates observed in this study in that the rates were initially rapid before slowing significantly after 20–100 h. Schroeder and Lee (9) have also reported a strongly nonlinear rate of Cr(III) oxidation by an unspecified type of $\text{MnO}_2(\text{s})$.

pH and Cr(III) Concentration. The rates of aqueous Cr(VI) formation for solutions with pH between 3.0 and 4.7 are shown in Figure 2a for 9.6×10^{-6} M Cr(III) solutions. At pH 3.0, there appeared to be a slight increase in the rate of Cr(III) oxidation, but at higher pH the oxidation rates were not significantly different (Figure 2a). Results (not shown here) from experiments with a lower $\beta\text{-MnO}_2(\text{s})$ surface area to solution volume ratio of $7.1 \text{ m}^2\text{-L}^{-1}$ showed indistinguishable differences in Cr(III) oxidation rates over a similar pH range. However, the

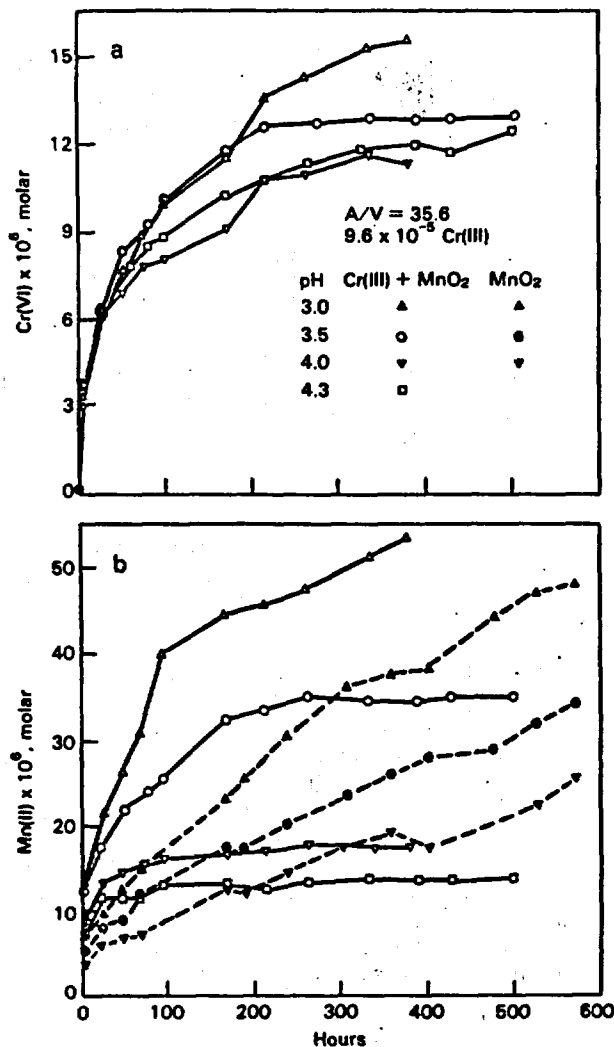


Figure 2. Effects of pH on the rates of (a) Cr(VI) formation and (b) β -MnO₂(s) dissolution (open symbols) for initial [Cr(III)] = 9.6×10^{-5} M. Solid symbols indicate rates of β -MnO₂(s) dissolution measured in Cr-free solutions.

parallel rate of β -MnO₂(s) dissolution measured during the oxidation rate experiments was markedly increased in the lower pH solutions (Figure 2b). Also, in Figure 2b, the rates of β -MnO₂(s) dissolution in the Cr-containing solutions (open symbols) are compared to the rates of purely acidic β -MnO₂(s) dissolution that were measured in Cr-free solutions (solid symbols) for comparable pH and surface area to solution volume ratios. Murray (15) has shown that MnO₂(s) dissolves more rapidly in low-pH solutions. Rates of β -MnO₂(s) dissolution were significantly more rapid for an initial period in the Cr solutions but eventually slowed with increasing time to rates that were less than those measured in the Cr-free solutions in which the rates of β -MnO₂(s) dissolution were observed to be approximately linear over long periods (Figure 2b). This result implies that an initial reaction between Cr(III) and β -MnO₂(s) increases the rate of β -MnO₂(s) dissolution above that caused purely by the acidic dissolution of β -MnO₂(s). However, after a period of rapid reaction, the Cr(VI) reaction products result in a decrease in the reactivity of β -MnO₂(s) and a consequent decrease in the rates of both Cr(III) oxidation and β -MnO₂(s) dissolution.

Rates of Cr(III) oxidation at pH 4.0 and $A/V = 35.0$ m²-L⁻¹ for a range of initial Cr(III) concentrations indicate a similar effect of the dissolved Cr on the rate of β -MnO₂(s) dissolution (Figure 3). The oxidation rates of Cr(III) were

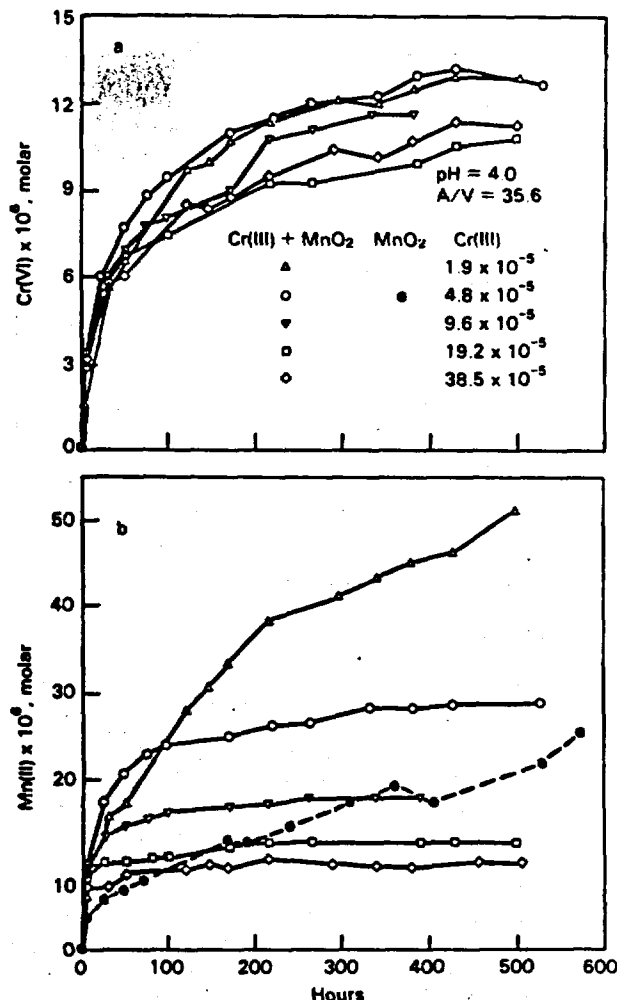


Figure 3. Effects of initial Cr(III) concentration on the rates of (a) Cr(VI) formation and (b) β -MnO₂(s) dissolution (open symbols) for pH 4.0 and $A/V = 35.6$ m²-L⁻¹. Solid symbols indicate the rate of β -MnO₂(s) dissolution measured in a pH 4.0, Cr-free solution.

not increased by increasing the initial Cr(III) concentration but were remarkably similar in magnitude as indicated by the increases in Cr(VI) concentrations (Figure 3a). In contrast, the overall rate of β -MnO₂(s) dissolution was decreased by increasing the initial Cr(III) concentration (Figure 3b). The rate of acidic β -MnO₂(s) dissolution in a Cr-free solution at pH 4.0 is also included in Figure 3b. A comparison of this rate to those in Cr solutions (Figure 3b) shows that concentrations of Mn increase in a linear manner in the absence of dissolved Cr species but are increased initially and then slowed in the Cr solutions, as was observed in previously described experiments (Figure 2b). The eventual depression in the initially rapid rates of Cr(III) oxidation and β -MnO₂(s) dissolution may be caused by a slow rate of desorption of the produced Cr(VI) species from the β -MnO₂(s) surfaces. The zero point of charge for β -MnO₂(s) is reported to occur at pH 7.3 (± 0.2) (16), thus the anionic Cr(VI) species (HCrO₄⁻ and CrO₄²⁻) are likely to be strongly adsorbed in acidic solutions. The direct adsorption of Cr(VI) species onto β -MnO₂(s) was found to be increased greatly as pH was lowered from 8.0 to 2.0 in adsorption experiments that are not reported here. We speculate that the strong adsorption of the anionic Cr(VI) species reduces the number of active sites on the β -MnO₂(s) surface, thus causing a decrease in the reaction rates for both Cr(III) oxidation and β -MnO₂(s) dissolution over time as the Cr(VI) concentration increases. Various surface reactions between Cr and Mn redox species are

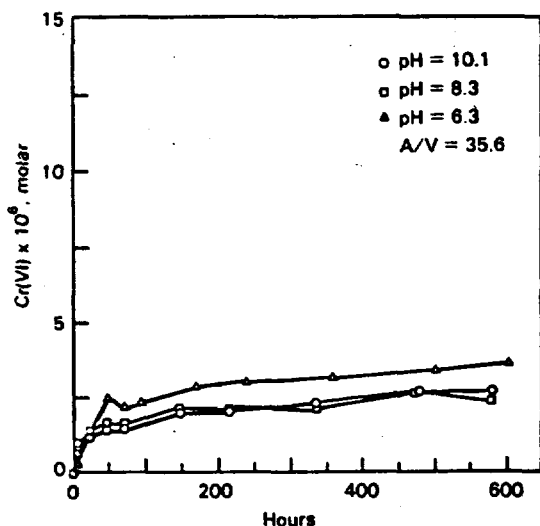


Figure 4. Rates of Cr(VI) formation in solutions containing the equivalent of 9.6×10^{-5} M Cr(III) precipitated as $\text{Cr}(\text{OH})_3(\text{s})$ with $A/V = 35.6 \text{ m}^2\text{-L}^{-1}$.

possible, and it is difficult to separate clearly their effects on reaction rates from those caused by adsorption processes on the basis of these experiments. However, considering the adsorption behavior of the anionic Cr(VI) species under acidic conditions, we expect that adsorption and desorption reactions are important for controlling the rate of Cr(III) oxidation for the experimental conditions described here.

Cr(III) Precipitation. In addition to the rate experiments conducted in acidic solutions, three experiments at pH 6.3, 8.3, and 10.1 were also conducted. The equivalent of 9.6×10^{-5} M aqueous Cr(III) was initially added to each of the solutions, but a whitish green solid was immediately precipitated, and the aqueous Cr(III) concentrations decreased to low levels. These observations, along with the solubility data for $\text{Cr}(\text{OH})_3(\text{s})$ of Rai et al. (1), indicated that Cr(III) was precipitated as $\text{Cr}(\text{OH})_3(\text{s})$. This precipitate was allowed to age for 2–3 days before 5.0 g of $\beta\text{-MnO}_2(\text{s})$ was added to the suspensions to begin the oxidation rate experiments. Although the solubility of $\text{Cr}(\text{OH})_3(\text{s})$ was expected to severely limit the Cr(III) concentration between pH 6.3 and pH 11.0, some oxidation of the available Cr(III) to Cr(VI) by $\beta\text{-MnO}_2(\text{s})$ was observed to take place (Figure 4). In neutral to basic solutions, anionic Cr(VI) species are less strongly adsorbed onto the $\beta\text{-MnO}_2(\text{s})$ surfaces, and all of the Cr detected in the solutions was determined to be hexavalent. Oxidation had increased the total Cr concentrations [(2–3) $\times 10^{-6}$ M] to levels above what would be expected from $\text{Cr}(\text{OH})_3(\text{s})$ solubility for this pH range [1.4×10^{-7} M, Rai et al. (1)]. The dissolved Mn concentrations were below the detection level. In qualitative terms, aqueous Cr(III) oxidation at intermediate pH may involve the buffering of Cr(III) to low but constant concentration by $\text{Cr}(\text{OH})_3(\text{s})$ solubility, followed by adsorption of some of the aqueous Cr(III) onto the $\beta\text{-MnO}_2(\text{s})$ surfaces, subsequent oxidation to Cr(VI), and desorption in these near-neutral to alkaline solutions. Unfortunately, the low solubility of $\text{Cr}(\text{OH})_3(\text{s})$ placed analytical limitations on the amount of rate information that could be obtained from these experiments. However, the experiments do indicate that the oxidation of aqueous Cr(III) at intermediate pH can result in total dissolved Cr concentrations that are above what might be predicted from $\text{Cr}(\text{OH})_3(\text{s})$ solubility.

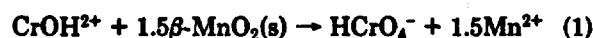
Reaction Stoichiometry. In the simplest case, the reaction between Cr(III) and $\beta\text{-MnO}_2(\text{s})$ to produce Cr(VI)

Table I. Reaction Stoichiometries Calculated from Slopes of Plots of Mn(II) versus Cr(VI) by Least-Squares Regression of the Rate Data from Figures 2 and 3

no. of points	pH	Cr(III), M	slope, Mn(II)/Cr(VI) ^a	R ² , %
9	3.0	9.6×10^{-5}	3.17 ± 0.54	97.6
11	3.5	9.6×10^{-5}	2.53 ± 0.24	98.9
9	4.0	9.6×10^{-5}	0.69 ± 0.16	95.6
11	4.3	9.6×10^{-5}	0.40 ± 0.14	89.8
10	4.0	1.9×10^{-4}	5.06 ± 0.74	97.9
11	4.0	4.8×10^{-5}	1.53 ± 0.18	98.6
9	4.0	9.6×10^{-5}	0.69 ± 0.16	95.6
9	4.0	19.2×10^{-5}	0.59 ± 0.18	92.3
9	4.0	38.5×10^{-5}	0.28 ± 0.20	74.4

^aError limits indicate two standard deviations.

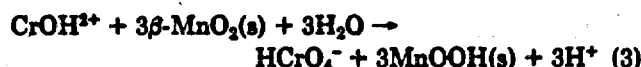
can be expressed by the following reaction, which is relevant to the experimental pH range of 3.0–4.7 (1), i.e.



Plots of dissolved Mn versus Cr(VI) (as HCrO_4^-) were made with the solution data from Figures 2 and 3 in an attempt to compare the experimental results to the stoichiometry of reaction 1. After an initial time period of nonlinearity for 20–100 h, these plots did show linear relationships between dissolved Mn(II) and dissolved Cr(VI), but the slopes, which should be indicative of the reaction stoichiometry, varied with pH and with Cr(III) concentration (Table I). At pH 3.0 and 3.5, the slopes were significantly higher than the 1.5 mol of Mn(II) to 1.0 mol of Cr(VI) ratio predicted by reaction 1 (Table I), indicating that the acidic dissolution of $\beta\text{-MnO}_2(\text{s})$, i.e.



occurred as a parallel reaction at these low pH values. More rapid dissolution of $\beta\text{-MnO}_2(\text{s})$ was evident in the lower pH solutions (see Figure 2b). At higher pH, the measured stoichiometry did decrease but to values lower than the 1.5 value indicated from reaction 1 (Table I). A similar trend of decreasing Mn to Cr(VI) ratio with increasing Cr(III) concentration was also evident for a single pH of 4.0 (Table I). A possible explanation for these observations of changing reaction stoichiometry with solution composition may be the formation of $\text{MnOOH}(\text{s})$ as the reduction product of $\beta\text{-MnO}_2(\text{s})$ at higher pH and higher Cr(III) concentration instead of Mn^{2+} as follows:



The formation of $\text{MnOOH}(\text{s})$ has been observed on particles of birnessite that were reacted with Co(II) to form Co(III) at pH 6.5 by Crowther et al. (11), and $\text{MnOOH}(\text{s})$ is known to be an intermediate product in the oxidative reaction pathway between aqueous Mn(II) and the final product of $\text{MnO}_2(\text{s})$ (17). However, the formation of $\text{MnOOH}(\text{s})$ was not directly observed in our experiments and must be viewed as speculative at the present time. Additionally, in studies of the oxidation of Fe(II) by birnessite (18), the formation of $\text{MnOOH}(\text{s})$ was ruled out, and deviations in the measured stoichiometries from the postulated reactions leading to $\text{MnOOH}(\text{s})$ formation were attributed to the adsorption of Fe(II) onto the birnessite and associated ferric hydroxide reaction products. In our studies, the adsorption of Cr(VI) species may have slightly affected the measured concentration ratios at early times before the adsorption capacity of $\beta\text{-MnO}_2(\text{s})$ was reached.

However, adsorption would seem to be an unlikely cause of such large differences in the apparent reaction stoichiometries because of the relatively small differences in total Cr(VI) adsorption that would be likely to occur over the range of acidic pH used in the experiments (3.0–4.7), which is far from the zero point of charge for $\beta\text{-MnO}_2(\text{s})$ [pH 7.3 (16)]. Also, the possibility exists that Mn(III) rather than Mn(IV) species on the $\beta\text{-MnO}_2(\text{s})$ surface is the dominant oxidant under some conditions. Clearly, the combined processes of Cr(III) oxidation, Cr(VI) adsorption, Mn redox speciation, and $\beta\text{-MnO}_2(\text{s})$ acidic dissolution make the determination of the reaction stoichiometries of oxidation–reduction reactions that occur at the surfaces of manganese oxides extremely difficult. Our data indicate that a combination of reactions is probable under acidic conditions.

Empirical Rate Expression. The experimental observations of (1) highly nonlinear reaction rates, (2) the lack of strong dependence on pH or Cr(III) concentration, and (3) the depression of $\beta\text{-MnO}_2(\text{s})$ dissolution rate in Cr solutions compared to Cr-free solutions indicate that the slow desorption of anionic Cr(VI) species from the $\beta\text{-MnO}_2(\text{s})$ surface is an important rate-limiting step for Cr(III) oxidation by $\beta\text{-MnO}_2(\text{s})$ in acidic solutions. Adsorption of Cr(VI) species was found to occur in acidic solutions and appeared to cause eventual decreases in the Cr(III) oxidation rate possibly by limiting the generation of new reactive sites on the $\beta\text{-MnO}_2(\text{s})$ surface. As a result, the Cr(III) oxidation rate was apparently more dependent on Cr(VI) concentration than on Cr(III) concentration. An empirical rate expression has been derived to account for the rate-limiting effect of the produced Cr(VI) species and is described below. This expression is only applicable to acidic solutions for which we have the most rate data. In neutral and basic solutions, the precipitation of $\text{Cr}(\text{OH})_3(\text{s})$ and the weaker adsorption of Cr(VI) species onto $\beta\text{-MnO}_2(\text{s})$ would require a different approach, but the small amount of rate data gathered for such conditions prevents us from formulating an applicable expression.

The rates of heterogeneous reactions that involve complex phenomena at mineral surfaces can be described, in some instances, by expressions that relate the reaction rate to the reaction affinity, which can be practically described by the differences between steady-state reactant concentrations and actual concentrations to some power (19). To apply such a rate expression to the rate of Cr(VI) formation, it is necessary to define a steady-state Cr(VI) concentration. However, in all the rate experiments, the concentrations of Cr(VI) continued to slowly increase, even after as long as 500 h, and steady-state concentrations were never convincingly reached. To derive a rate expression, we assumed that all of the aqueous Cr(III) in the experimental solution would be oxidized to Cr(VI) by reaction with $\beta\text{-MnO}_2(\text{s})$, given sufficient time and $\beta\text{-MnO}_2(\text{s})$. Because the rate of Cr(III) oxidation is dependent on the amount of Cr(VI) produced, we express this assumption in terms of the fraction of Cr(VI) to total dissolved Cr remaining in solution, f_{Cr} , by the following limit:

$$f_{\text{Cr}} = [\text{Cr(VI)}]/[\text{Cr(VI)} + \text{Cr(III)}] \rightarrow 1.0 \text{ as } t \rightarrow \infty \quad (4)$$

where the brackets refer to molar concentrations and t is time in seconds. Using this assumption, we propose that the following rate expression is descriptive of the rate of Cr(III) oxidation to Cr(VI) by reaction with $\beta\text{-MnO}_2(\text{s})$:

$$df_{\text{Cr}}/dt = k(A/V)[\text{Cr}_t]^{-1}(1.0 - f_{\text{Cr}})^n \text{ for } f_{\text{Cr}} \leq 1.0 \quad (5)$$

where k is a rate constant with units of $\text{mol}\cdot\text{m}^{-2}\cdot\text{s}^{-1}$, $[\text{Cr}_t]$ refers to the total dissolved Cr concentration (i.e., $[\text{Cr(VI)}]$

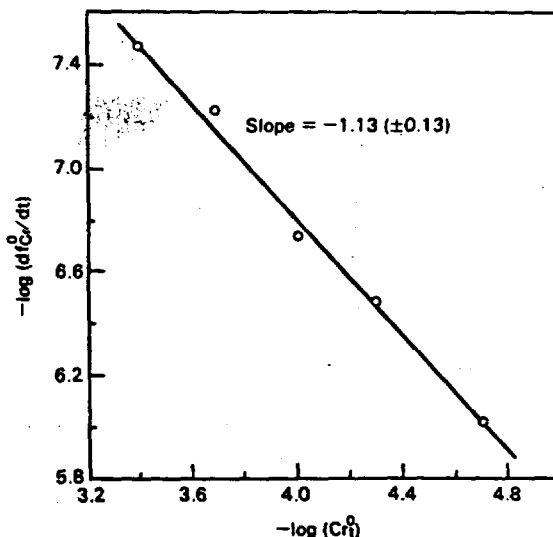


Figure 5. log-log plot showing the inverse dependence of the fractional rate of Cr(VI) formation on the concentration of total Cr. The slope was calculated by least-squares regression, and the error limits indicate two standard deviations about the slope.

+ Cr(III)], and n is some positive number. By describing the rate in terms of the fractional rate of Cr(VI) formation in eq 5, the rate-limiting effects caused by the adsorption of the Cr(VI) products onto $\beta\text{-MnO}_2(\text{s})$ are empirically taken into account. The inverse dependence on $[\text{Cr}_t]$ is a result of describing the rate in terms of f_{Cr} but is also confirmed by the determination of a slope of approximately -1 for a plot of the logarithm of the initial fractional rate of Cr(VI) formation (df_{Cr}^0/dt) versus the logarithm of the initial total Cr concentration $[\text{Cr}_t^0]$ (Figure 5). The rates plotted in Figure 5 were derived by normalizing the Cr(VI) concentration data shown in Figure 3a to total Cr concentration to obtain f_{Cr} at successive times. The initial rates were determined by fitting second-order polynomials to the f_{Cr} versus time data by a least-squares method and taking the derivatives of those polynomials at time equal to zero.

The rate expression in eq 5 can be integrated with respect to time and f_{Cr} to give

$$1/(1 - f_{\text{Cr}})^{n-1} - 1/(1 - f_{\text{Cr}}^0)^{n-1} = (n-1)[\text{Cr}_t]^{-1}(A/V)kt \quad (6)$$

where f_{Cr}^0 is the initial fraction of Cr(VI) to total Cr. Equation 6 expresses the relationship between f_{Cr} and the time that should be observed in the rate experiments if the proposed rate expression is valid. To use eq 6 to evaluate the rate of aqueous Cr(VI) formation, it is necessary to determine the value of n , the empirical order of the reaction. The value of n was determined from two sets of initial rate experiments that are described below, and this value was tested against the rate data from longer term experiments with eq 6 to determine the accuracy of the rate expression.

The initial rate method as applied to this study involves the determination of the fractional rate of Cr(VI) formation as a function of the initial ratio of Cr(VI) to total dissolved Cr (f_{Cr}^0). These initial rates, if linear, can be thought of as tangential lines along the reaction pathway as f_{Cr} increases nonlinearly with time. We assumed that the anionic Cr(VI) species, which were added to solution to create specific values of f_{Cr}^0 in the fractional rate experiments, immediately caused a rate-limiting effect because of the reduction of reaction affinity through adsorption onto $\beta\text{-MnO}_2(\text{s})$ just as if they were produced by

Table II. Summary of Initial Fractional Rates of Cr(VI) Formation as a Function of f_{Cr}^0 *

f_{Cr}^0	pH	$df_{Cr}^0/dt \times 10^{10}$ ^b	R^2 , %
0.0	3.0	2.7 (± 0.6)	95.6
0.05	3.0	2.3 (± 0.2)	99.4
0.10	3.0	1.9 (± 0.3)	98.4
0.20	3.0	1.9 (± 0.2)	96.8
0.40	3.0	0.6 (± 0.2)	93.4
0.0	4.0	3.2 (± 0.6)	97.2
0.05	4.0	2.6 (± 0.3)	98.9
0.10	4.0	1.9 (± 0.4)	96.4
0.20	4.0	1.4 (± 0.2)	98.2
0.30	4.0	1.0 (± 0.2)	97.1
0.40	4.0	0.5 (± 0.2)	89.7

* $A/V = 71.3 \text{ m}^2\text{-L}^{-1}$. ^b Error limits indicate two standard deviations.

Cr(III) oxidation. If the initial reaction rate for fractional Cr(VI) production, df_{Cr}^0/dt , is linear with time, then n can be determined from a plot of $\log(df_{Cr}^0/dt)$ versus $\log(1 - f_{Cr}^0)$ as follows from the logarithmic form of eq 5, i.e.

$$\log(df_{Cr}^0/dt) = \log\{k(A/V)[Cr_t]^{-1}\} + n \log(1 - f_{Cr}^0) \quad (7)$$

The value of n was determined from such a log-log plot by using the rate data obtained from two sets of experiments conducted at pH 3.0 and 4.0 in which the fractional rates of Cr(VI) formation were measured in separate experiments with specific values of f_{Cr}^0 , that ranged from 0.0 to 0.40. The possibility exists that the apparent rate-limiting effects of Cr(VI) may decrease at higher values of f_{Cr}^0 , possibly because of greater saturation of adsorption sites on $\beta\text{-MnO}_2(\text{s})$, but the extremely slow reactions rates under such conditions prevented the gathering of accurate data.

The fractional rate experiments lasted a total of 6-8 h, during which a total of 8-10 samples were withdrawn and analyzed to determine the change in the quantity $f_{Cr} - f_{Cr}^0$ with time. The change in $f_{Cr} - f_{Cr}^0$ with time was observed to be linear for each experiment for the 6-8-h period; hence, the initial fractional rates were determined from the slopes calculated by linear regressions of the experimental data of $f_{Cr} - f_{Cr}^0$ at $(A/V)t$ and are given in Table II. The quantity A/V was included in the independent variable for the rate calculations because of the change in solution volume that occurs during a rate experiment as solution samples are removed. We assumed that the surface area of $\beta\text{-MnO}_2(\text{s})$ did not change significantly. Least-squares regressions of the log-log plot defined by eq 7 gave slopes of 2.9 (± 0.8) and 3.5 (± 0.6) (Figure 6), and the value of n is taken to be the average of the two slopes, 3.2 (± 0.8). In Figure 6, it is clear that there are some large errors associated with the rate data. These errors reflect scatter in the rate data and are a result of analytical difficulties encountered in determining the small changes in Cr(VI) concentrations that occurred during some of the fractional rates experiments conducted in solutions with the higher values of f_{Cr}^0 , such as 0.30 and 0.40.

The magnitude of the rate constant, k , was determined from eq 6 rearranged as

$$[1/(1 - f_{Cr})^{2.2} - 1/(1 - f_{Cr}^0)^{2.2}]/\{2.2(A/V)[Cr_t]^{-1}\} = kt \quad (8)$$

A value for k for each rate experiment conducted in acidic solution was determined from the slopes of plots of the left side of eq (8) versus t , and these values of k are listed in Table III. Using the average k from all of the experiments, the rate expression describing the fractional rate of Cr(VI)

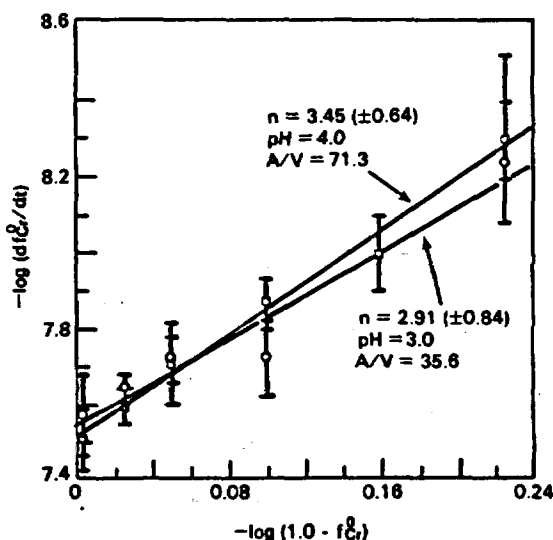


Figure 6. log-log plot of the fractional rate of Cr(VI) formation showing the slopes used to determine n . The error limits indicate two standard deviations about the slopes.

Table III. Summary of Experimental Conditions, Rate Constants, and Linear Correlation Coefficients (9-11 Data Points of Regression Analyses)

pH	$[Cr_t] \times 10^5$	A/V	$k \times 10^{12}$ ^a	R^2 , %
4.0	1.9	35.6	1.3 (± 0.1)	98.3
4.0	4.8	35.6	2.5 (± 0.9)	85.4
4.0	9.6	35.6	2.1 (± 0.8)	86.9
4.0	19.2	35.6	1.2 (± 0.5)	82.9
4.0	38.5	35.6	1.3 (± 0.5)	84.6
3.0	9.6	35.6	3.3 (± 0.8)	93.0
3.5	9.6	35.6	1.8 (± 0.8)	81.1
4.3	9.6	35.6	1.6 (± 0.6)	82.3
3.0	9.6	7.1	2.3 (± 0.6)	90.8
3.5	9.6	7.1	2.3 (± 0.7)	90.1
4.0	9.6	7.1	3.0 (± 0.8)	87.6
4.4	9.6	7.1	2.8 (± 2.0)	84.4
4.7	9.6	7.1	2.4 (± 1.0)	81.2
4.0	9.6	0.7	4.0 (± 1.9)	81.7
4.0	9.6	71.3	2.3 (± 0.7)	87.7
4.0	9.6	7.1	1.4 (± 0.5)	83.0
4.0	9.6	35.6	1.2 (± 0.5)	80.0
4.0	9.6	71.3	1.3 (± 0.5)	75.3

^a Error limits indicate two standard deviations. Average $k = 2.0 (\pm 1.6) \times 10^{-13} \text{ mol}\cdot\text{m}^{-2}\cdot\text{s}^{-1}$.

formation in acidic solutions can be written in final form as

$$df_{Cr}/dt = k(A/V)[Cr_t]^{-1}(1 - f_{Cr})^{3.2(\pm 0.8)} \text{ for } f_{Cr} \leq 1.0 \quad (9)$$

where

$$k = 2.0 (\pm 1.6) \times 10^{-13} \text{ mol}\cdot\text{m}^{-2}\cdot\text{s}^{-1} \quad (10)$$

Linear correlation coefficients, R^2 , are also listed in Table III to provide an indication of the linearity of the plots of the left side of eq 8 versus t . The R^2 values range from 75 to 98% for 9-11 data points, indicating that the empirically derived rate expression given in eq 9 is generally descriptive of the reaction rates observed in the experiments with acidic solutions.

The rate expression in eq 9 can be used to calculate the time required to oxidize a specific amount of Cr(III) to Cr(VI). If we consider a hypothetical example of a 1.0-kg mass of an acidic waste material containing 0.05 wt % $\beta\text{-MnO}_2(\text{s})$ with a specific surface area of $5 \text{ m}^2\cdot\text{g}^{-1}$ and a saturated porosity of 20%, then the resulting surface area to volume ratio for $\beta\text{-MnO}_2(\text{s})$ is $10 \text{ m}^2\cdot\text{L}^{-1}$. With this value

Table IV. Time Required for Fractional Conversion of a 10^{-5} M Cr(III) Solution to Cr(VI) for 1 kg of a 20% Porosity Soil Containing 0.05 wt % β - $MnO_2(s)$ with a Specific Surface Area of $5.0 \text{ m}^2 \cdot \text{g}^{-1}$

f_{Cr}	days	f_{Cr}	days
0.10	7	0.50	95
0.30	31	0.90	4140

and the integrated form of the rate expression given by eq 8, the times required to oxidize 10, 30, 50, and 90% of a static 10^{-5} M Cr(III) solution are given in Table IV. Although this is a largely heuristic calculation, it points out the highly nonlinear nature of the oxidation reaction and indicates the long times needed to accomplish complete conversion of Cr(III) to Cr(VI). In flowing systems involving short residence times and acidic, oxygen-saturated leachates, such as at some coal fly ash disposal sites, only small amounts of Cr(III) may be converted to Cr(VI) by reaction with β - $MnO_2(s)$ before leachates encounter reducing conditions in the underlying soils where Cr(VI) would be reduced to Cr(III) and possibly precipitated as $Cr(OH)_3(s)$ depending on pH (1). However, we expect that other forms of manganese oxides may cause more rapid rates of Cr(III) oxidation, and the calculations shown in Table IV represent a base-line case for which future comparisons might be made.

Conclusions

Our experiments indicate that the oxidation of aqueous Cr(III) does not occur by surface-catalyzed reactions with dissolved oxygen but by direct reaction with β - $MnO_2(s)$, although the exact reaction stoichiometry is complicated by the parallel rate of acidic β - $MnO_2(s)$ dissolution and possible formation of intermediate manganese oxide reaction products such as $MnOOH(s)$. The extent of Cr(III) oxidation is limited probably by anionic Cr(VI) adsorption in acidic solutions and by $Cr(OH)_3(s)$ precipitation in neutral to alkaline solutions. It is important to note, however, that soil forms of $MnO_2(s)$ are likely to have lower zero points of charge [e.g., pH 2.3 for δ - $MnO_2(s)$ (15) versus 7.3 for β - $MnO_2(s)$ (16)] and higher surface energies, implying that these forms may cause more rapid oxidation of Cr(III) than the β - $MnO_2(s)$ used here. The high solubilities of Cr(VI) solids in oxidizing environments imply that Cr may be attenuated only by adsorption reactions rather than by precipitation of a solubility-controlling solid. The ready oxidation of Cr(III) to Cr(VI) by manganese oxides indicates the need to examine the mineralogy and oxidation potential of both the waste materials and the underlying soils at sites where Cr-bearing wastes may be deposited. The presence of manganese oxides would indicate the potential for greater transport of aqueous Cr as Cr(VI) species in groundwaters, whereas in the absence

of manganese oxides the oxidation of aqueous Cr(III) is unlikely to occur.

Acknowledgments

We thank I. P. Murarka, EPRI project manager, for his continual support and interest. We thank B. Sass, J. Schramke, and two anonymous reviewers for their comments and discussions and Jan Baer for her editorial review.

Registry No. MnO_2 , 1313-13-9; Cr, 7440-47-3.

Literature Cited

- (1) Rai, D.; Sass, B. M.; Moore, D. A. *Inorg. Chem.* 1987, 26, 345-349.
- (2) Sass, B. M.; Rai, D. *Inorg. Chem.* 1987, 26, 2228-2232.
- (3) Benjamin, M. M.; Hayes, K. F.; Leckie, J. O. J. *Water Pollut. Control Fed.* 1982, 54, 1472-1481.
- (4) Espenson, J. H.; King, E. L. *J. Am. Chem. Soc.* 1963, 85, 3328-3333.
- (5) Smillie, R. H.; Hunter, K.; Loutit, M. *Water Res.* 1981, 15, 1351-1354.
- (6) Stollenwerk, K. G.; Grove, D. B. *J. Environ. Qual.* 1985, 14, 396-398.
- (7) Murray, J. W. *Geochim. Cosmochim. Acta* 1975, 39, 505-519.
- (8) Bartlett, R.; James, B. *J. Environ. Qual.* 1979, 8, 31-35.
- (9) Schroeder, D. C.; Lee, G. F. *Water, Air, Soil Pollut.* 1975, 4, 355-365.
- (10) Nakayama, E.; Kawamoto, T.; Tsurubo, S.; Fuginaga, T. *Anal. Chim. Acta* 1981, 130, 401-404.
- (11) Crowther, D. L.; Dillard, J. G.; Murray, J. W. *Geochim. Cosmochim. Acta* 1983, 47, 1399-1403.
- (12) Oscarson, D. W.; Huang, P. M.; Liaw, W. K.; Mammer, V. T. *Soil Sci. Soc. Am. J.* 1983, 47, 644-648.
- (13) Rai, D.; Zachara, J. M.; Eary, L. E.; Girvin, D. C.; Moore, D. A.; Resch, C. T.; Sass, B. M.; Schmidt, R. L. "Geochemical Behavior of Chromium Species"; final report EA-4544; Electric Power Research Institute: Palo Alto, CA, 1986.
- (14) Skougstad, M. W.; Fishman, M. J.; Friedman, L. C.; Erdman, D. E.; Duncan, S. S. *Methods for Determination of Inorganic Substances in Water and Fluvial Sediments*; U.S. Geological Survey: Washington, DC, 1979; Book 5, pp 337-340.
- (15) Murray, J. W. *J. Colloid Interface Sci.* 1974, 46, 357-371.
- (16) Healy, T. W.; Herring, A. P.; Fuerstenau, D. W. *J. Colloid Interface Sci.* 1966, 21, 435-444.
- (17) Hem, J. D.; Lind, C. J. *Geochim. Cosmochim. Acta* 1983, 47, 2037-2046.
- (18) Postma, D. *Geochim. Cosmochim. Acta* 1985, 49, 1023-1033.
- (19) Lasaga, A. C. In *Kinetics of Geochemical Processes*; Lasaga, A. C., Kirkpatrick, R. J., Eds.; Mineralogical Society of America: Washington, DC, 1981; Chapter 1.

Received for review November 25, 1986. Accepted July 20, 1987. This research was funded by the Electric Power Research Institute (EPRI) under Contract RP2485-03, titled "Chemical Attenuation Studies".